Dually guided-mode-resonant graphene perfect absorbers with narrow bandwidth for sensors

2016 J. Phys. D: Appl. Phys. 49 32LT01

(http://iopscience.iop.org/0022-3727/49/32/32LT01)

Letters
IOP Publishing
Journal of Physics D: Applied Physics
J. Phys. D: Appl. Phys. 49 (2016) 32LT01 (5pp)
doi:10.1088/0022-3727/49/32/32LT01

Letter

Dually guided-mode-resonant graphene perfect absorbers with narrow bandwidth for sensors

Yongbing Long[1], **Yuanxing Li**[2], **Liang Shen**[3], **Wenyue Liang**[2], **Haidong Deng**[1] and **Haitao Xu**[1]

[1] College of Electronic Engineering, South China Agricultural University, Guangzhou, 510642, People's Republic of China
[2] School of Applied Physics and Material, WuYi University, Jiangmen, 529020, People's Republic of China
[3] State Key Laboratory on Integrated Optoelectronics, College of Electronic Science and Engineering, Jilin University, 2699 Qianjin Street, Changchun 130012, People's Republic of China

E-mail: yongbinglong@126.com

Received 21 May 2016, revised 9 June 2016
Accepted for publication 20 June 2016
Published 19 July 2016

CrossMark

Abstract

Dually guided-mode-resonant graphene perfect absorbers are numerically proposed by placing graphene grips on dielectric subwavelength grating that is backed by one-dimensional photonic crystals (1DPCs). By optimizing parameters of the grating, perfect absorption with a narrow bandwith of 1.1 nm is achieved at a wavelength of 632.8 nm. The perfect absorption is attributed to the dual excitation of the guided-mode resonance of both the grating and the 1DPCs. When this type of absorber is used in refractive index sensors, the figure of merit reaches as high as 124, a value much higher than that of the sensors based on metal perfect absorbers. In addition, it is observed that a slight change of the refractive index in the surrounding environment causes large intensity variation of reflection at a fixed wavelength; accordingly, high index sensitivity is achieved for the sensors.

Keyword: perfect absorption, dually guided-mode resonance, graphene, sensors

S Online supplementary data available from stacks.iop.org/JPhysD/49/32LT01/mmedia

(Some figures may appear in colour only in the online journal)

1. Introduction

Perfect absorbers have attracted increasing attention due to their potential application to thermo and solar power harvesting, sensing and detecting [1–7]. In particular, perfect absorption occurring in sensors can help to significantly improve the sensitivity of devices due to the large modulation depth [8–11]. In 2010, Liu *et al* experimentally presented a refractive index sensor which was equipped with infrared perfect absorbers with a metal–dielectric–metal configuration [8]. The sensing capability of this device is improved up to four times that of the conventional plasmonic sensors due to the low reflection caused by perfect absorption. More recently, Lu *et al* designed a narrow-band perfect absorber consisting of metal periodic nanoslits [9]. The full width at half maximum (FWHM) of the absorption peak is as narrow as 8 nm, and the sensing figure of merit (FOM) reaches as high as 25, while previous sensors based on other metal nanostructures have only achieved a FOM that is less than 10 [12–14]. Apparently, designing perfect absorbers with narrower bandwidth can improve FOM of the sensors since FOM is inversely proportional to the bandwidth [9, 10]. However, the bandwidth of metal perfect absorbers (or absorbers with metal nanostructures) is limited by the inherent metal loss and still remains relatively broad [8–14], which severely hampers further improvement of sensing properties for sensors.

Meanwhile, recent studies have presented graphene perfect absorbers (GPAs) with narrow bandwidth by combining graphene with dielectric nanostructures [15–18]. For example, Piper *et al* have achieved GPAs by placing a graphene layer on a photonic crystal slab with one-dimensional photonic crystals (1DPCs) acting as a Bragg mirror [15]. Perfect absorption with a FWHM of 14 nm is achieved at a wavelength of 1500 nm by critically coupling the guided-mode resonances of the photonic crystal slab to the graphene. More recently, Grande *et al* sandwich a single graphene between dielectric grating and spacer/1DPCs (i.e. Bragg mirror), and total absorption is achieved due to the guided-mode resonance of the grating [18]. In this study, the FWHM of the guided-mode-resonant GPAs is reduced to 4.4 nm. The value is much narrower than that (>8 nm) of the absorbers based on metal nanostructures [8–14]. With both narrow bandwidth and perfect absorption, better sensing properties can be expected when the GPAs are integrated into sensors. However, previous studies have mainly focused on how to achieve perfect absorption [15–18]; few of them have investigated whether the guided-mode-resonant GPAs can be incorporated into sensors to achieve better sensing capability. The 1DPCs in these studies have only acted as a reflecting mirror, and the guided-mode resonance of 1DPCs has not been excited or investigated.

This paper numerically proposes dually guided-mode-resonant GPAs in water and investigates the sensing performance of this type of perfect absorber when they are used in refractive index sensors. For this purpose, guided-mode-resonant GPAs are first constructed by placing graphene grips on dielectric subwavelength grating that is backed by 1DPCs. By optimizing parameters of the device, the guided-mode resonances of both the grating and the 1DPCs are simultaneously excited. Correspondingly, perfect absorption with a narrower FWHM of 1.1 nm is achieved and a high FOM of 124 is obtained for the sensors. The value of FOM is much higher than that (less than 25) of the sensors based on metal nanostructures [8–14].

2. Structure and method

The structure for the proposed dually guided-mode-resonant GPAs is shown in figure 1, in which a periodic graphene strip array is placed on a subwavelength TiO_2 grating and the grating is supported by 1DPCs. The thickness, period and strip width of the subwavelength gratings are h, p and w, respectively. The 1DPCs are composed of 10 pairs of (SiO_2/TiO_2). To calculate light absorption in graphene grips, the finite element method is first employed to calculate the optical electric field by setting the left and right boundaries of the computational domain as periodic boundary conditions and the top and bottom as perfectly matched layers [19]. With

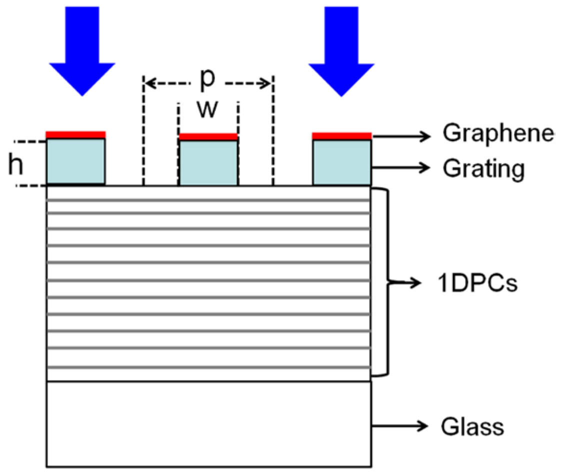

Figure 1. Structure of the guided-mode-resonant GPAs. p, w and h respectively denote period, strip width and thickness of the subwavelength gratings.

the optical electric field as input parameters, light absorption in $A(\lambda) = \int_{x \in \text{layer}} \omega \varepsilon_0 k n |E(x)|^2 / I(\lambda) \mathrm{d}x$ [20], where ε_0 is the permittivity of vacuum; λ and $I(\lambda)$ are respectively the wavelength and intensity of the incident light; n and k denote the refraction index and extinction coefficient of graphene; $E(x)$ is the electrical optical field in graphene. In the calculation, the refractive indexes of TiO_2 and SiO_2 are assumed to be 2.5 and 1.5. The graphene is assumed to be 0.34 nm and the refractive index is estimated to be $n = 3.0 + \mathrm{i}C_1\lambda/3$ with $C_1 = 5.446\ \mu\mathrm{m}^{-1}$ [21].

3. Results and discussion

To obtain dually guided-mode-resonant GPAs, light absorption in the monolayer graphene strips is first optimized by tailoring the parameters (h, p and w) of the grating. The optimization process mainly includes two parts. First, the Monte Carlo method is used to calculate the light absorption of graphene strips in the devices with the parameters (h, p and w) randomly distributed in a broad range. With this method, we can achieve a series of parameters (h, p and w) of the grating where light absorption shows local maximum values. Second, these parameters obtained by Monte Carlo simulation are used as initial values to achieve optimized device parameters by calculating light absorption of graphene as a function of h, p and w. In the calculation, the devices are assumed to be immersed in water with a refractive index of 1.332 and the incident light is assumed to be TE-polarized and the wavelength is set as the emission wavelength (i.e. 632.8 nm) of the He–Ne laser. The thickness of TiO_2 and SiO_2 layers in 1DPCs is respectively set as 60 nm and 100 nm so that the wavelength of the incident light is positioned in the photonic bandgap of 1DPCs and the 1DPCs have a high reflection of 100% at the wavelength of 632.8 nm. After careful optimization, light absorption in the graphene strips reaches 99.3% with a FWHM of 1.1 nm when p, w and h of the grating are respectively set as 421.3, 151.6

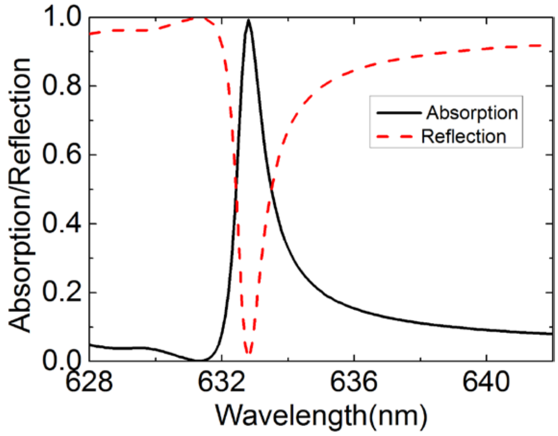

Figure 2. Absorption and reflection spectra of graphene strips in device I.

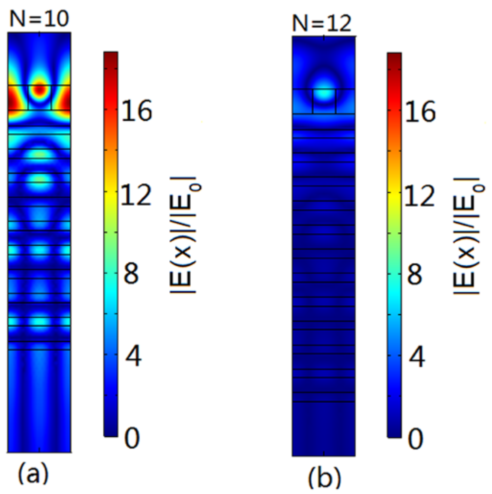

Figure 3. Optical electric field in device I with varied N. (a) $N = 10$; (b) $N = 12$. $|E(x)|$ denotes the modulus of the optical electric field in the device and $|E_0|$ denotes that of the incident light.

and 167.1 nm, and the device with these parameters is called device I. The calculated results are shown in figure 2.

The total absorption in graphene strips is investigated by calculating the distribution of the optical electric field in device I and the calculated results are shown in figure 3(a). The two main results can be observed from the figure. First, a large optical electric field is confined within the strips of the grating. This is partly attributed to the excitation of the guided-mode resonance of the grating. When the parameters of the grating are properly designed, phase matching between the guided mode of the grating and the incident light is enabled and consequently the guided-mode resonance of the grating is excited, which leads to significant improvement of the optical electric field both inside and around the strips of grating [15–18]. Second, large optical electric field is also found to be confined in the 1DPCs and at the interface between the 1DPCs and the substrates. This should be attributed to the excitation of the guided-mode resonance of the 1DPCs [22–24], which occurs when the reciprocal lattice vector of the grating is equal to the wavevector of the guided mode of the 1DPCs. The excited guided mode is simultaneously

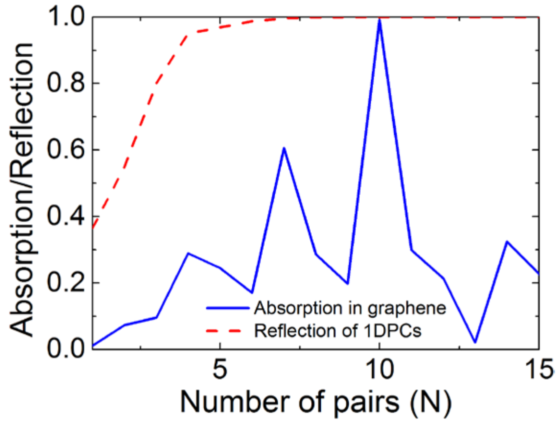

Figure 4. Absorption as a function of the pair layers (N) of (SiO_2/TiO_2) in 1DPCs. The red dashed line denotes the reflection of the 1DPCs.

modulated by the periodic modulation of refractive index in the 1DPCs and the periodicity of dielectric grating. As a result, the optical electric field resonates at both the parallel and perpendicular direction to the incident light, which in turn improves the optical electric field both inside and around the 1DPCs (see figure 3(a)). The excited guided-mode resonance of both the grating and the 1DPCs can leak evanescent waves to the interface of grating/air and subsequently improve the light–graphene interaction. As the external leakage energy of this type of dually guided-mode resonance is equal to the intrinsic loss of graphene strips, critical coupling occurs and perfect absorption is achieved in the graphene strips.

The optical performance of the dually guided-mode-resonant GPAs is further investigated by calculating light absorption as a function of the pair layers (N) of (SiO_2/TiO_2) in 1DPCs. In the calculation, N is increased from 1 to 15 and the results are shown in figure 4, where light absorption shows an oscillating behavior with the increase in N. Perfect absorption in graphene is achieved only when N is set as 10, but the absorption is reduced rapidly when N increases or decreases although the reflection of 1DPCs remains a high value of 100%. GPAs in this case are found to be different from those obtained by exciting solely the guided-mode resonance of the grating[4]. For the latter, light absorption in graphene rises to 100% when N is increased from 1 to 10 and remains a constant value of 100% with any further increase in N (see figure S3 in the supplementary material (stacks.iop.org/JPhysD/49/32LT01/mmedia)). This is because 1DPCs in this type of guided-mode-resonant GPA only act as a mirror to reflect light back for re-absorption and have little effect on the pattern of the optical electric field in the device when N increases (see figure S2). More details concerning this type of GPA is shown in the supplementary material[4].

For the dually guided-mode-resonant GPAs proposed in this paper, however, the case is different since the guided-mode resonance of the 1DPCs is another important factor contributing to the improvement of light absorption in

[4] See supplementary material at stacks.iop.org/JPhysD/49/32LT01/mmedia for the GPAs obtained by exciting only the guided-mode resonance of the grating.

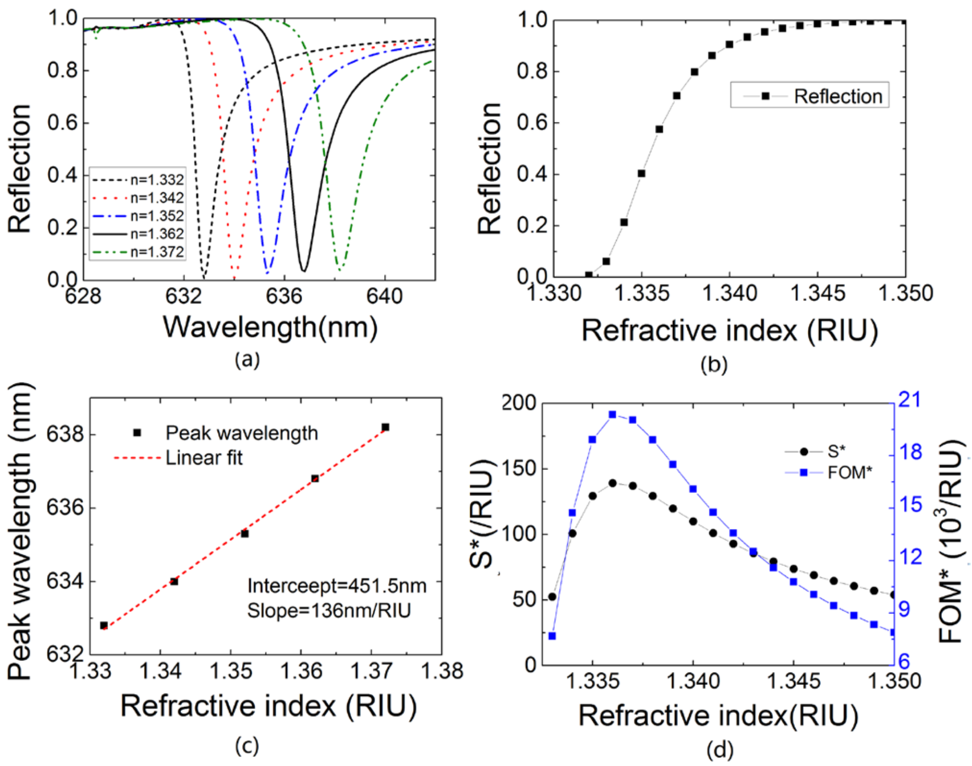

Figure 5. (a) Reflection spectra of the guided-mode-resonant GPAs with varied refractive index of the surrounding environment. (b) Reflection at the wavelength of 632.8 nm as a function of the refractive index of the surrounding environment. (c) Spectral position of the reflection dips as a function of refractive index of the environment. (d) S^* and FOM* of the guided-mode-resonant GPAs.

graphene. When N is changed, the wavevector of the guided mode of the 1DPCs varies and is no longer equal to the reciprocal lattice vector of the grating [22–24]. Consequently, the guided-mode resonance of the 1DPCs can not be excited and the optical electric field in 1DPCs turns very weak, as shown in figure 3(b). Less energy is leaked from the guided-mode resonance of the 1DPCs into the grating. The optical electric field in the grating is found to be obviously reduced when compared with figure 3(a) where the guided-mode resonance of the 1DPCs is excited. Correspondingly, external leakage energy of the dually guided-mode resonance is reduced and light absorption in graphene decreases rapidly although reflection of the 1DPCs remains 100% with N equal to 12, as shown in figure 4. The finding indicates that the excitation of the guided-mode resonance of the 1DPCs is an essential criterion to achieve absorption enhancement in graphene for the GPAs proposed in this paper.

Finally, we examine whether the dually guided-mode-resonant GPAs can be incorporated into sensors to detect refractive index. For this purpose, we first calculate light absorption in graphene when the refractive index of the surrounding environment of device I is set as different values. In the calculation, the surrounding refractive index is varied from 1.332 to 1.372 with a step of 0.01. The calculated reflection spectra are shown in figure 5(a), where obvious redshift of reflection dip is observed when the refractive index increases. Additionally, figure 5(b) demonstrates that reflection at the wavelength of 632.8 nm rapidly rises from 0.007 to 0.9 when the refractive index is increased from 1.332 to 1.340. These results indicate that optical performance of the dually guided-mode-resonant GPAs is ultrasensitive to the refractive index of the surrounding environment. The graphene absorbers can be used in sensors to detect refractive index.

The sensing capability of refractive index sensors is usually described by the following equations [9–12]:

$$S = \Delta\lambda/\Delta n,\ \mathrm{FOM} = S/\mathrm{FWHM},\ S^* = \Delta I/\Delta n,\ \mathrm{FOM}^* = S^*/I \quad (1)$$

where S denotes spectral sensitivity and FOM denotes figure of merit when spectral shift is measured; Δn and $\Delta\lambda$ are the changes of the refractive index and the spectral shift of the reflection spectra; FWHM is the bandwidth of the reflection spectra; ΔI is the change of light intensity at a fixed wavelength and I is the absolute light intensity; FOM* represents the intensity-sensing capability when the measurement of the reflective light is intensity.

According to the equations above, we first evaluate the sensing capability of the GPAs by calculating S and FOM. The calculated results are shown in figure 5(c). The slope of the curve in the figure shows the sensitivity S reaches 136 nm/RIU. A high FOM of 124 is also achieved, a value much higher than that of the sensors (less than 25) based on nanostructures reported in recent studies [8–14]. The relatively high sensing capability should be attributed to the narrow bandwidth (about 1.1 nm) of the GPAs in water. As a result of the narrow bandwidth, a slight change of refractive index will cause a large reflection variation for a given wavelength, as shown in figure 5(b). With these reflection data as inputs, S^* and FOM* are calculated by using equation (1) and the calculated results are shown in figure 5(d). It is found that a high value of 142/RIU is achieved for the sensitivity S^* at a fixed wavelength of 632.8 nm and FOM* reaches a much higher value of 20036/RIU. Both the values of S^* and FOM* are much larger than those obtained from the perfect absorber sensors based on metallic nanostructures [8–14]. More importantly, the value of S^* is also higher than that of the widely used refractive index sensors based on the prism-coupled surface plasmon resonance of thin metal films [25]. Thus, it can be expected that sensors based on dually guided-mode-resonant GPAs would have better sensing performance in the potential applications such as chemical and biomedical sensing, as well as imaging techniques for sensing which measure the reflectivity changes at a given wavelength caused by the refractive index variation [25, 26].

4. Conclusion

In summery, we propose dually guided-mode-resonant GPAs by placing graphene grips on dielectric subwavelength grating that is backed by 1DPCs. When parameters of the subwavelength grating and the 1DPCs are properly adjusted, perfect absorbers with narrow bandwidth of 1.1 nm are obtained at a wavelength of 632.8 nm. The perfect absorption with narrow bandwidth is attributed to the dually guided-mode resonance of both the grating and the 1DPCs. Due to the excitation of the guided-mode resonance of 1DPCs, light absorption in graphene strips shows an oscillating behavior when the pair layers (N) of (SiO_2/TiO_2) in 1DPCs increases and perfect absorption is achieved only when N is equal to 10. When this type of GPAs is used in refractive index sensors, a high FOM of 124 is achieved, which is 5 times that (i.e. 25) of the sensors based on metal perfect absorbers [8–10]. In addition, it is observed that a small increase (only 0.008 RIU) in the refractive index of the surrounding environment can rapidly raise the reflection of the sensor from 0.007 to 0.9. Accordingly, high values of 142/RIU and 20036/RIU are achieved for S^* and FOM* of the sensors. These values are also much higher than those of the sensors based on metal nanostructures [8–14]. The results presented in this paper suggest that incorporating the dually guided-mode-resonant GPAs into refractive index sensors is an efficient method to achieve high sensing properties for the devices.

Acknowledgments

This work is supported by Guangdong Natural Science Funds for Distinguished Young Scholar (Grant No: 2014A030306005), Natural Science Foundation of Guangdong Province, China (Grant No. S2013010012854, 2016A03031339), Foundation for High-level Talents in Higher Education of Guangdong Province, China (Yue Cai-Jiao [2013]246, Jiang Cai-Jiao [2014]10), Development Program for Outstanding Young Teachers in Guangdong University (Yue Jiaoshi [2014]108), The Science and Technology Program of Guangzhou (No. 201607010176).

References

[1] Landy N I, Sajuyigbe S, Mock J J, Smith D R and Padilla W J 2008 *Phys. Rev. Lett.* **100** 207402
[2] Li S J, Gao J, Cao X Y, Zhang Z, Zheng Y J and Zhang C 2015 *Opt. Express* **23** 3523
[3] He J N, Ding P, Wang J Q, Fan C Z and Liang E J 2015 *Opt. Express* **23** 8670
[4] Zhou W C, Li K W, Song C, Hao P, Chi M B, Yu M X and Wu Y H 2015 *Opt. Express* **23** A413
[5] Long Y B, Su R M, Wang Q W, Shen L, Li B W and Zheng W H 2014 *Appl. Phys. Lett.* **104** 091109
[6] Maier T and Brueckl H 2010 *Opt. Lett.* **35** 3766–8
[7] Dao T D, Chen K, Ishii S, Ohi A, Nabatame T, Kitajima M and Nagao T 2015 *ACS Photonics* **2** 964–70
[8] Liu N, Mesch M and Weiss T 2010 *Nano Lett.* **10** 2342–8
[9] Lu X Y, Zhang L Y and Zhang T Y 2015 *Opt. Express* **23** 20715
[10] Lu X Y, Zhang L Y and Zhang T Y 2015 *Opt. Express* **23** 29842
[11] Jamali A A and Witzigmann B 2014 *Plasmonics* **9** 1265
[12] Ameling R, Langguth L, Hentschel M, Mesch M, Braun P V and Giessen H 2010 *Appl. Phys. Lett.* **97** 253116
[13] Ye J and Dorpe P V 2011 *Plasmonics* **6** 665–71
[14] Huang C, Ye J, Wang S, Stakenborg T and Lagae L 2012 *Appl. Phys. Lett.* **100** 173114
[15] Piper J R and Fan S H 2014 *ACS Photonics* **1** 347
[16] Hu J H, Huang Y Q, Duan X F, Wang Q, Zhang X, Wang J and Ren X M 2014 *Appl. Phys. Lett.* **105** 221113
[17] Xiang Y J, Dai X Y, Guo J, Zhang H, Wen S C and Tang D Y 2014 *Sci. Rep.* **4** 5483
[18] Grande M *et al* 2015 *Opt. Express* **23** 21032
[19] Long Y B, Li Y X and Su R M 2014 *AIP Adv.* **4** 087143
[20] Long Y B 2010 *Sol. Energy Mater. Sol. Cells* **94** 744–9
[21] Bruna M and Borini S 2009 *Appl. Phys. Lett.* **94** 031901
[22] Robertsona W M and May M S 1999 *Appl. Phys. Lett.* **74** 1800
[23] Liscidini M and Sipe J E 2009 *J. Opt. Soc. Am.* B **26** 279
[24] Chen Y, Shi J, Liu T, Dong J, Zhu Q and Chen W 2015 *Phys. Lett.* A **379** 2257–60
[25] Shalabney A and Abdulhalim I 2011 *Laser Photonics Rev.* **5** 571–606
[26] Homola J, Yee S S and Gauglitz G 1999 *Sensors Actuators* B **54** 3–15